applied sciences

MDPI

Article

Stress and Deformation Analysis of the Foundation of a Large High-Temperature Molten-Salt Storage Tank

Jinmeng Qiao, Caifu Qian and Zhiwei Wu *

College of Mechanical and Electrical Engineering, Beijing University of Chemical Technology, Beijing 100029, China
* Correspondence: zwzhiweiwu@163.com

Abstract

Concentrating solar power (CSP) is a promising renewable energy technology, and molten-salt storage tanks are core equipment for ensuring its stable operation, where the foundation plays a decisive role in the structural design and safe service of the tanks. To address the lack of systematic stress and deformation analysis for large high-temperature molten-salt storage tank foundations, this study aims to investigate the mechanical and thermal behaviors of the foundation under actual operating conditions. A numerical simulation method was adopted to perform stress and deformation analysis on the foundation of a large high-temperature molten-salt storage tank. The results show that the maximum von Mises stress of 229.26 MPa is concentrated on the steel plate of the foundation. The radial deformation of the foundation was calculated, and the maximum radial deformation reaches 36.64 mm, which provides an important reference for the design of both the foundation and the entire molten-salt storage tank. Under the given internal pressure and operating temperature, the height of the molten salt has a significant impact on the radial deformation of the foundation. Additionally, ambient temperature variations from −28.7 °C to 20 °C exert little influence on the temperature distribution of the foundation, indicating that the thermal insulation performance of the tank is excellent. The findings of this study can provide theoretical support for optimizing the design and operation strategies of molten-salt storage tanks, particularly their foundations.

Keywords: molten-salt storage tank; foundation; stress and deformation analysis; numerical simulation

1. Introduction

As the core energy storage equipment in concentrating solar power (CSP) systems, molten-salt storage tanks feature structural safety considerations, thermal protection performance, and mechanical behavior under high-temperature and complex working conditions, which directly determine the operational reliability and economy of the power plant. Efficient thermal insulation and design are critical to ensuring their long-term stable operation. The development of relevant technologies not only promotes the upgrading of the solar thermal industry but also provides important support for next-generation reactor technology [1–3]. As molten-salt storage tanks are usually large in size and complex in structure as well as load, numerical simulations about stress and deformation analysis based on the finite element method are often performed for tank design or safety assessment. Wan et al. conducted research on the thermal and mechanical properties of molten-salt thermal storage tanks. The research results showed that the radiation heat transfer effect in the gas

Check for updates

Academic Editors: Juan García Rodríguez and Paolo Renna

Received: 4 March 2026
Revised: 16 April 2026
Accepted: 25 April 2026
Published: 29 April 2026

Copyright: © 2026 by the authors. Licensee MDPI, Basel, Switzerland. This article is an open access article distributed under the terms and conditions of the Creative Commons Attribution (CC BY) license.

phase space inside the tank causes the tank top temperature to tend towards consistency with the molten-salt temperature, resulting in the tank wall temperature remaining basically constant at different molten-salt levels, thereby making the heat loss of the tank not change with the salt level. At the same time, the study found that the thermal deformation of the tank is significant. Any form of constraint imposed on this thermal deformation may induce extremely high thermal stress, posing a serious threat to the safe operation of the tank [4]. Gao et al. measured temperature and molten-salt inventory levels in a high-temperature tank at a 50 MW central receiver CSP plant and numerically evaluated the thermal and mechanical properties of a molten-salt thermal energy storage tank. Results show that larger temperature gradients and thermal stresses are primarily localized along the tank floor edge and the air–salt interface. Notably, the maximum thermal stress at the tank edge is three times higher than that at the interface. Thermal load significantly affects tank deformation, particularly at the roof edge. Despite the large variation in molten-salt levels, tank wall temperatures and displacements present a minor change [5]. Zhang et al. constructed an experimental system using a new molten salt to study temperature distribution during cooling (550–180 °C). They observed 200 mm stratification at the tank bottom with a maximum temperature difference of 161 °C at the lower edges. The foundation temperature peaked at the upper-middle part and decreased radially. Heat loss dropped from 3.65 kWh to 1.82 kWh as the temperature fell to 310 °C, and the effect of stratification on bottom heat loss was analyzed [6]. Odenthal et al. addressed the issue of bending stresses in large-sized high-temperature tanks with thermal stratification. With the help of experimentally validated numerical methods, it was revealed that a low thermocline thickness can be a limiting factor for large tank diameters. The temperature has a major influence on the maximum possible tank size [7]. Li and Zhang established an integrated model of the finite volume method (FVM) and finite element method (FEM) for a molten-salt single-tank system with a composite wall. The effects of the operating parameters and structural parameters on the cyclic dynamic thermal and mechanical characteristics were investigated. Their study findings suggested that to improve the thermal efficiency of a single tank and guarantee its security, the inlet flow rate and inlet/outlet temperature differences should be controlled within a certain range [8]. Wang et al. established a numerical model for a molten-salt thermocline tank with multi-layer wall structure and performed CFD-based thermo-mechanical parametric analysis considering eight influencing factors. The results show that the inlet velocity, cold salt temperature, porous bed porosity, and filler particle properties significantly affect discharging performance. Increasing the inlet velocity, cold salt temperature or filler specific heat or reducing the bed porosity, particle diameter or conductivity can thin the thermocline. Meanwhile, increasing the inlet velocity, cold salt temperature or firebrick thickness or decreasing the steel wall thickness, porosity, particle diameter, conductivity or specific heat reduces the maximum steel wall stress [9]. Tang and Tao modeled the cold and hot tanks of a 100 MW CSP plant in China. The materials and geometric models were determined based on related specifications and engineering experience. The mechanical characteristics of the tanks under steady conditions, including the deformation, stress distribution, and stress concentration, were simulated and calculated [10]. Ren et al. established thermal and stress analysis models for the molten-salt storage tank. A comprehensive thermal mechanical coupling model is constructed. Their study found the radial compressive stress on the outer surface reaches approximately 140 MPa, while the tank wall is primarily subjected to circumferential forces. The temperature exerts a negligible impact on the stress of the tank wall, yet it significantly affects its deformation [11]. Xue et al. modeled large-scale molten-salt storage tanks and their foundations for concentrated solar power plants, investigating their thermal performance under various conditions. The impacts of factors like ambient temperature, insulation thickness, expanded clay ag-

gregate thickness, and ventilation systems on temperature distribution and heat loss are analyzed. Their study provides valuable insights for optimizing the thermal performance of molten-salt storage tanks, advancing energy storage system design and application [12]. Jia et al. established a thermal analysis model for large-scale molten-salt heat storage tanks and investigated the effects of liquid level and heat storage temperature on temperature distribution and heat loss. The results indicate that the tank top inner surface exhibits a small temperature drop from the molten-salt due to radiation, while obvious temperature differences and gradients appear near the tank bottom annular plate. Tank bottom and top heat loss are barely affected by liquid level, with the top accounting for about 40% of total heat loss owing to thinner insulation [13]. Wang et al. proposed a two-dimensional discrete model (2DIM) using Modelica to analyze molten-salt temperature distribution and heat loss in two-tank thermal energy storage systems. They studied the effects of tank volume, liquid level, salt temperature, and heater layout on system performance. Results show that heating the gas inside the tank reduces heat loss by 25.89% and increases efficiency by 0.17%, providing a reference for the design and operation of TES tanks [14]. Tagle-Salazar et al. introduced an innovative transient modeling tailored for the comprehensive annual performance analysis of a solar tower power plant coupled to a two-tank TES system, incorporating molten salts as the storage medium. The obtained results demonstrate a favorable concurrence in the transient behavior of the performance parameters, considering the heat flows, state of charge, net power, and others, with a discrepancy of less than 1% in annual production when benchmarked against a commercial software reference. The occurrence of local heat loss primarily stems from distortions or imperfections within the construction, including the structure, insulation layers, or foundation, thereby creating thermal bridges between the storage fluid and the external ambient environment [15]. Chen et al. adopted a unidirectional thermo-mechanical coupling finite element method to analyze the thermal and mechanical performances of molten-salt thermal storage tanks in concentrated solar power plants. Results show that molten-salt level has little effect on heat loss, with tank wall heat loss accounting for 44.4% of the total, and operating temperature significantly raises thermal losses. Increasing bottom plate thickness improves deformation resistance; greater wall thickness exponentially reduces maximum stress and deformation, reaching 159.27 MPa at 35 mm. A concrete elastic modulus of 5 MPa minimizes base plate stress to 39.45 MPa, while a further decrease induces excessive settlement and stress rebound [16]. Du et al. designed a commercial-scale EPCM-TES tank suitable for a 50 MWe tower power station, established an integrated model coupling the finite volume method (FVM) and the finite element method (FEM), and considered real mechanical loads and cyclic temperature distributions in the stress analysis. The research showed that during the charging phase, when the tank wall is heated, creep damage initially occurs in the area above 4.4 m, and subsequent high-temperature EPCM filler further induces creep in the area below 4.4 m; whereas, during the discharging phase, the tank wall is cooled by cold salt, which can prevent creep damage throughout the entire height of the tank [17]. Gage et al. analyzed the mechanical properties of commercial-scale storage tanks for the new generation of molten chloride-based molten-salt thermal storage (CSP) technology and designed a water-cooled foundation to minimize thermo-mechanical stress [18].

However, the above studies mainly focus on the tank shell or overall structure, and lack systematic and quantitative analysis on the thermo-mechanical coupling behavior of the tank foundation, which has a complex layered structure and material composition, and is directly subjected to high temperature gradients and mechanical loads. Most investigations also ignore the influences of actual service conditions, including internal pressure, high-temperature molten salt, and ambient temperature variation, on the foundation's stress and deformation. The present work conducts a detailed thermo-mechanical coupling analysis

on the foundation of a large high-temperature molten-salt storage tank under realistic operating conditions, quantitatively evaluates the stress distribution and deformation characteristics, and identifies the key factors governing foundation performance. Compared with studies concentrating only on the tank shell, this work yields more comprehensive and engineering-targeted results, providing accurate data for the design and safety evaluation of tank foundations, which constitutes the main scientific novelty of this study.

2. Establishing a Numerical Model of the Molten-Salt Storage Tank

2.1. Structure and Parameters

The molten-salt storage tank consists of the shell, insulating layer, foundation and soil as shown in Figure 1. The diameter of the tank shell is 39 m, the height of the cylindrical shell is 19 m and the height of the foundation excluding the bottom soil is 1.9 m. The foundation of molten-salt storage tank is composed of several layers, with Figure 2 showing the schematic structure and Tables 1 and 2 listing the properties of the shell, insulating layer and the foundation layers. The material property data used in this study were obtained from the public technical literature and web-based material databases. The concrete grades used are C20 (C16/20) and C35 (C28/35) according to GB 50010 and Eurocode 2.

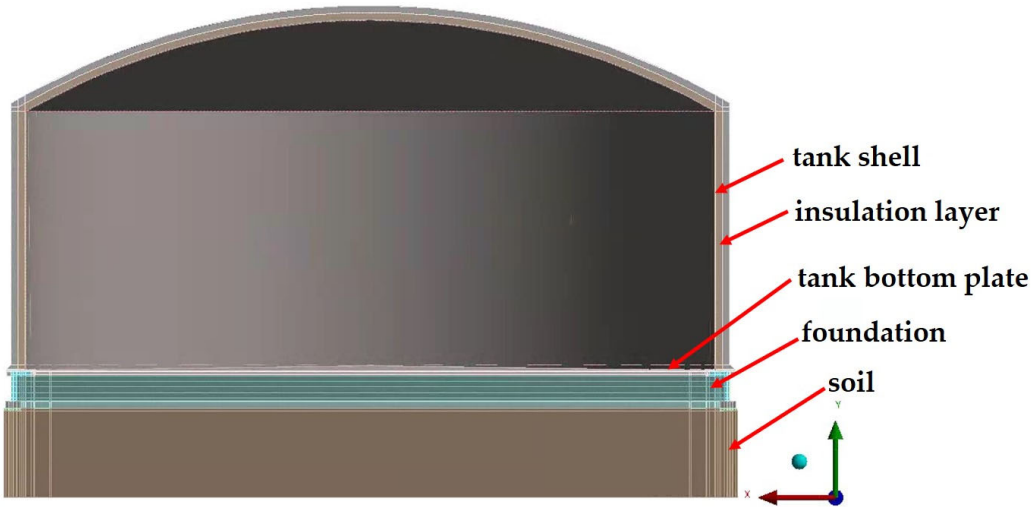


Figure 1. Schematic structure of the whole molten-salt storage tank.

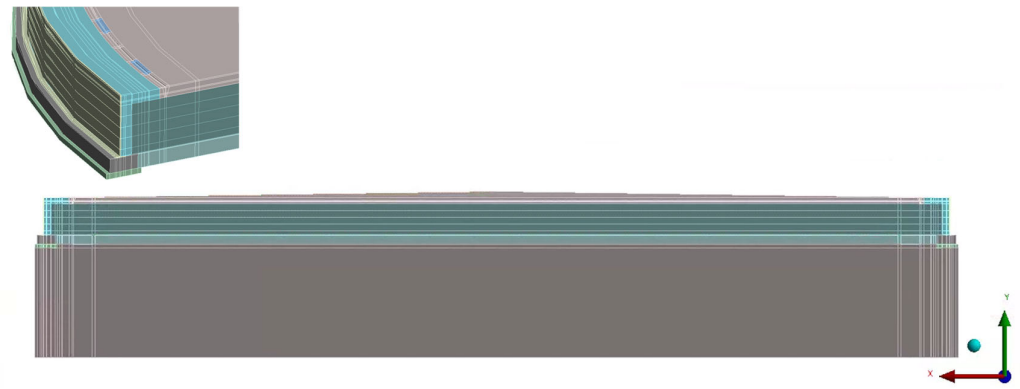


Figure 2. Schematic foundation structure of the molten-salt storage tank.

In this study, the SOLID185 element (ANSYS) was adopted. It is an 8-node linear brick element with three degrees of freedom per node, suitable for the 3D thermo-mechanical coupling analysis of solid structures. After performing the mesh independence test as listed in Table 3, the total node number is 1,102,389 and the total element number is 1,014,333.

The mesh models for the whole structure and foundation are shown, respectively, in Figures 3 and 4. This model employs a sequential thermo-mechanical coupling solution. The analysis software employed in this study is ANSYS 2022 R1.

Table 1. Material properties of the shell and foundation.

Materials	Density ($kg \cdot m^{-3}$)	Young Modulus (MPa)	Poisson's Ratio	Linear Expansion Coefficient (C^{-1})	Thermal Conductivity ($W \cdot (m \cdot K)^{-1}$)
Ceramic concrete	1600	840	0.27	5.83×10^{-6}	110 °C 0.1244 293 °C 0.1863 396 °C 0.2154 577 °C 0.2507
Calcium silicate	220	385	0.312	2.5×10^{-5}	100 °C 0.065 200 °C 0.075 300 °C 0.087 400 °C 0.1 500 °C 0.115 600 °C 0.13
C20	2400	26,000	0.27	1×10^{-5}	1.45
C35	2500	31,500	0.27	8.33×10^{-6}	1.45
Stainless steel	8030	20 °C 195,000 100 °C 189,000 150 °C 186,000 200 °C 183,000 250 °C 179,000 300 °C 176,000 350 °C 172,000 400 °C 169,000 450 °C 165,000 500 °C 160,000 550 °C 156,000	0.3	1.88×10^{-5}	45
Fine sand	1500	50	0.2	5×10^{-6}	0.4
Sandy soil	1500	50	0.2	5×10^{-6}	0.4
Fibrolite	2400	26,000	0.27	9×10^{-6}	2.04
Concrete pier	2500	31,500	0.27	1×10^{-5}	1.45

Table 2. Thermal conductivity of the insulation and soil.

Materials	Thermal Conductivity ($W \cdot (m \cdot K)^{-1}$)
Rock wool	$\lambda = 0.0337 + 0.000151T$ ($-20\ °C \leq T \leq 100\ °C$) $\lambda = 0.0395 + 4.71 \times 10^{-5}T + 5.03 \times 10^{-7}T^2$ ($100\ °C < T \leq 600\ °C$)
Aluminum silicate	$\lambda_0 = 0.044$ (70 °C) $\lambda_{L1} = \lambda_0 + 0.0002$ ($70 < T \leq 400\ °C$) $\lambda_{H1} = \lambda_{L1} + 0.00036 - (T - 400)$ ($T > 400\ °C$)
soil	20 °C 1.5 40 °C 2 50 °C 2.5 70 °C 4 90 °C 4.5

Table 3. The grid-independence test.

Mesh Count	Maximum Von Mises Equivalent Stress
761,655	308.15
1,014,333	310.31
1,865,532	315.28

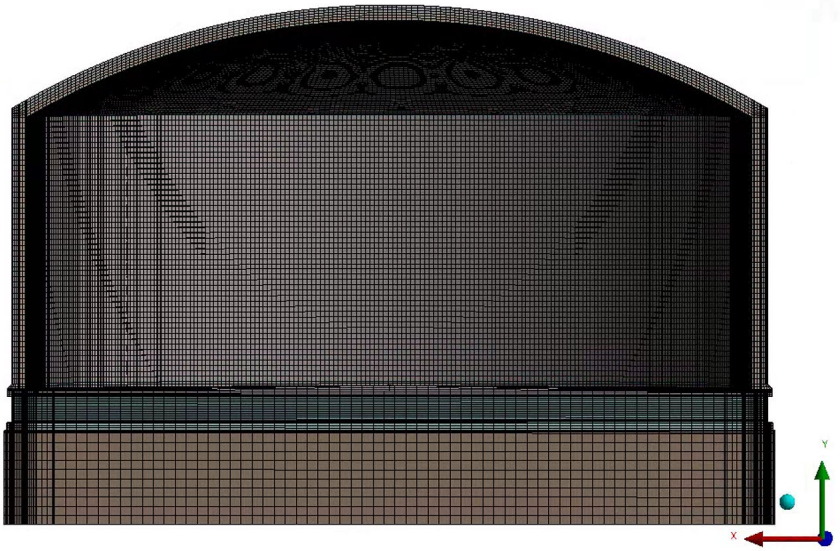


Figure 3. Mesh models for the whole molten-salt storage tank.

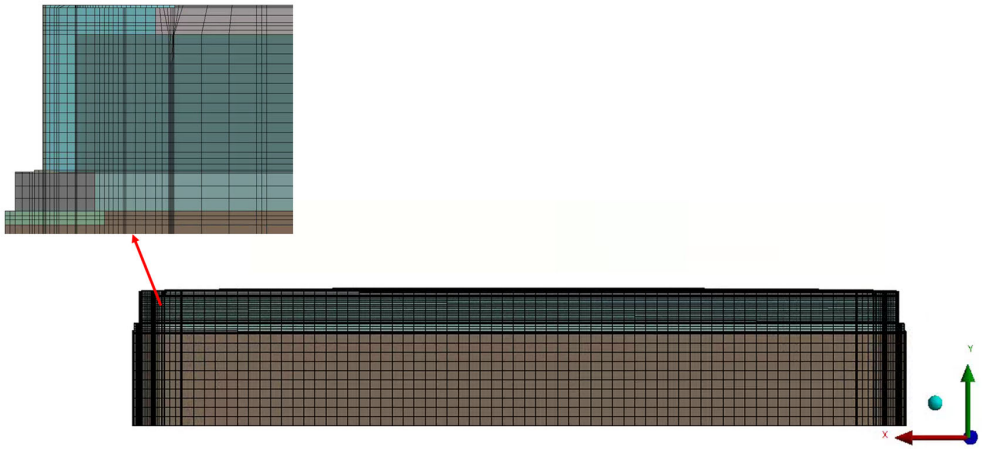


Figure 4. Grid model for the foundation of the molten-salt storage tank.

2.2. Loads and Boundary Conditions

(1) Loads

(1) Gravity load: Gravity acceleration is applied to the entire structure.
(2) Internal pressure: A uniform pressure of 0.002 MPa is applied on all internal surfaces.
(3) Hydrostatic pressure: Hydrostatic pressure proportional to the medium height (density = 1892.84 kg/m^3) is applied on the internal surface of the tank, as shown in Figure 5.
(4) Thermal loads: An operating temperature of 350 °C is applied on the internal surface; the ambient temperature is set to −28.7 °C; convective heat transfer with a coefficient of 7.35 W/(m^2·°C) is applied outside the insulation layer; the temperature at the bottom of the foundation soil is 5 °C, as illustrated in Figure 6.

(2) Contact conditions

Frictional contact is defined between each foundation layer with a friction coefficient of 0.5.

(3) Constraints

The bottom of the 5 m deep soil layer beneath the foundation is fixed (no displacement or rotation). This simplification is widely adopted in geotechnical simulations: it covers

the main stress influence zone, ignores negligible far-field effects, ensures computational efficiency, and yields conservative (safe) results that satisfy engineering accuracy.

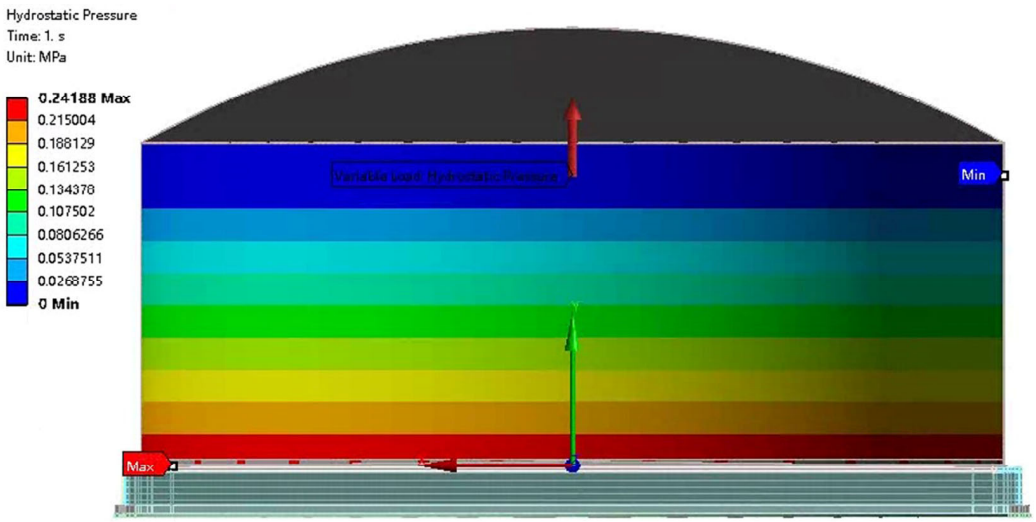


Figure 5. Application of hydrostatic pressure.

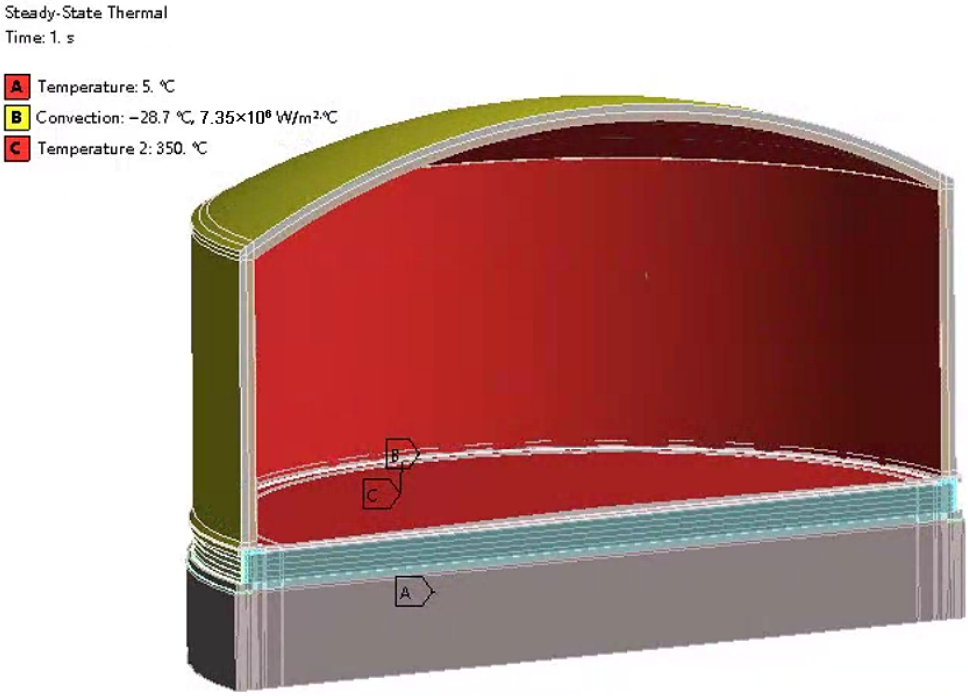


Figure 6. Application of thermal loads.

2.3. Load Cases

In practical operation, three load cases may be encountered, as listed in Table 4. But only load case 3 includes all loads and it turns out that this case is more critical than the other two cases. Thus, in this section, only the results of load case 3 were presented.

Table 4. Table of load cases.

Load Cases	Load
Load case 1	Gravity + thermal load
Load case 2	Gravity + internal pressure + hydrostatic pressure
Load case 3	Gravity + internal pressure + hydrostatic pressure + thermal load

3. Results and Discussion

As an extreme condition in load case 3, the operating pressure is 0.002 MPa, the molten-salt height is 12,000 mm, and the operating temperature is 400 °C. For the design of the molten-salt tank foundation, von Mises stress and radial deformation are particularly important; therefore, the discussion below focuses on the results under the extreme conditions of load case 3.

Figure 7 shows the temperature distribution of the whole molten-salt tank. Clearly, a temperature gradient was found at the foundation and it seems that the thermal insulation of the foundation is ideal. Figures 8 and 9 are the von Mises stress distributions of the whole tank and the foundation, respectively. It is seen that the largest von Mises stress at the foundation occurred in the bottom steel plate of the tank with the magnitude being 229.26 MPa, which is much smaller than the allowable stress of the steel plate.

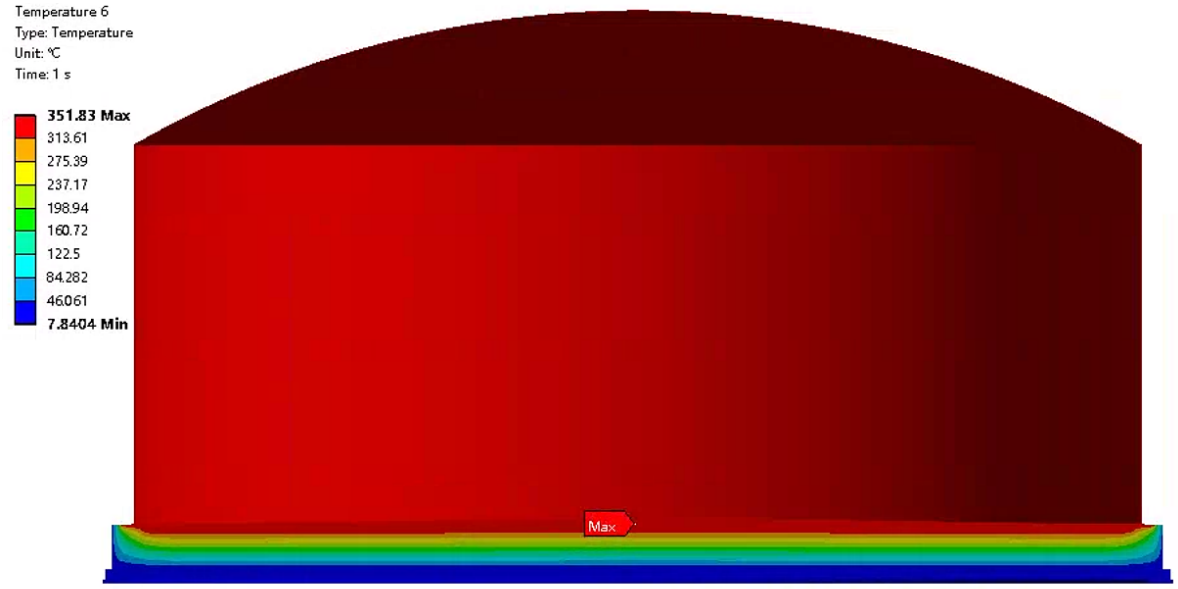


Figure 7. Temperature distribution of the whole molten-salt tank.

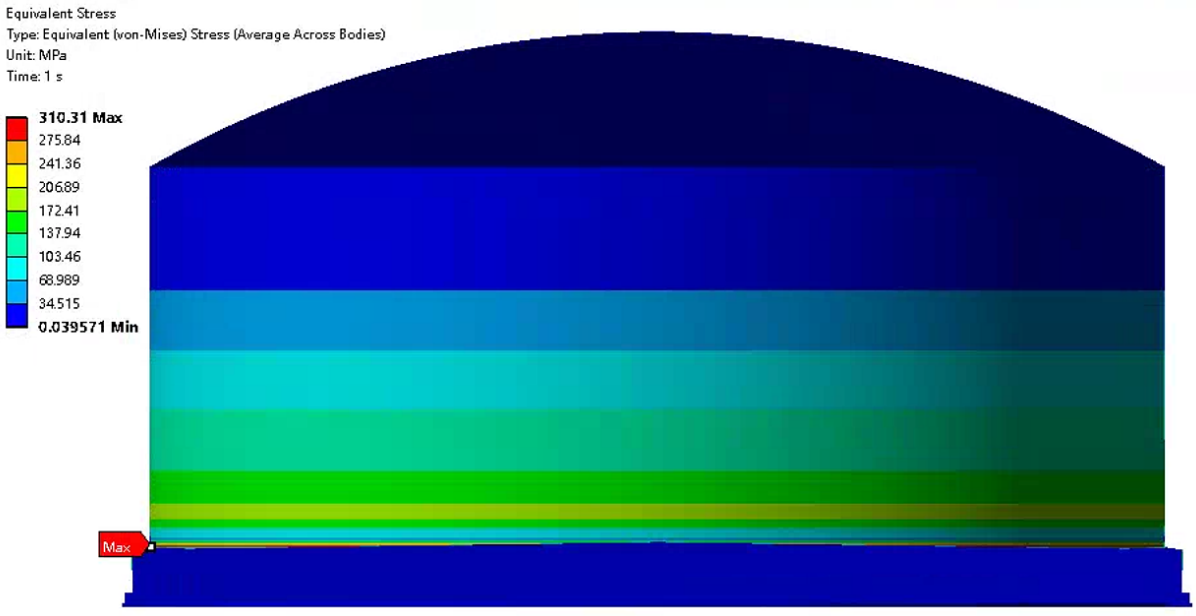


Figure 8. Von Mises stress contour of the whole molten-salt tank.

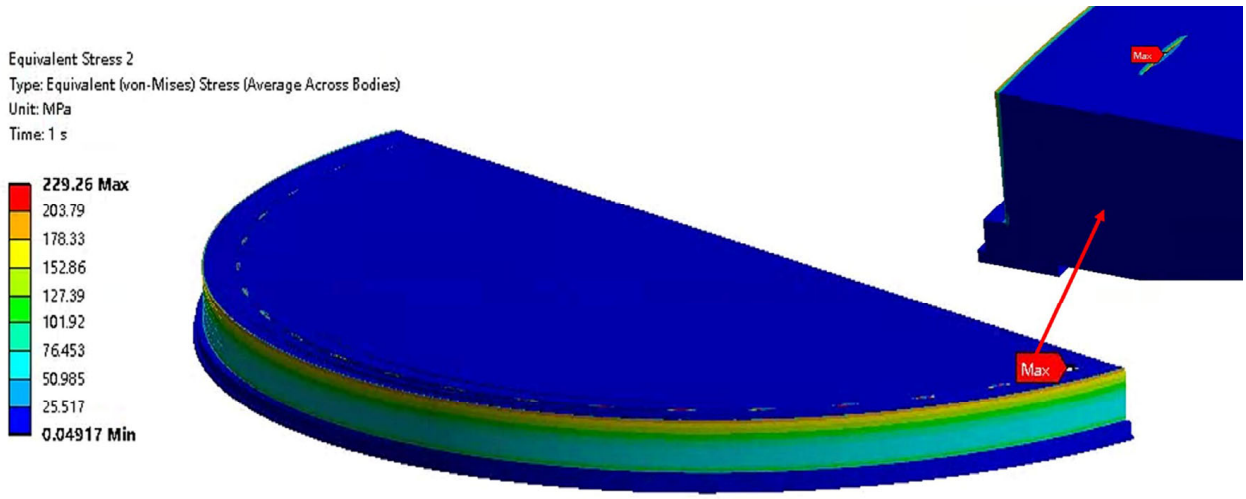


Figure 9. Von Mises stress contour of the foundation of the molten-salt tank.

Figures 10 and 11 show the radial deformation of the whole tank and the foundation, respectively. It is seen that the largest radial deformation of the foundation occurs at the edge of the sand soil layer, with a value of 36.64 mm. In engineering practice, a peripheral steel wall is arranged around the foundation. The diameter of the wall should consider the radial deformation of the tank and foundation to avoid excessive thermal stress. Moreover, the shear behavior between layers in the foundation is also related to the radial deformation of the foundation. Therefore, the radial deformation distribution obtained here is valuable for the structural design and material selection of both the tank and the foundation.

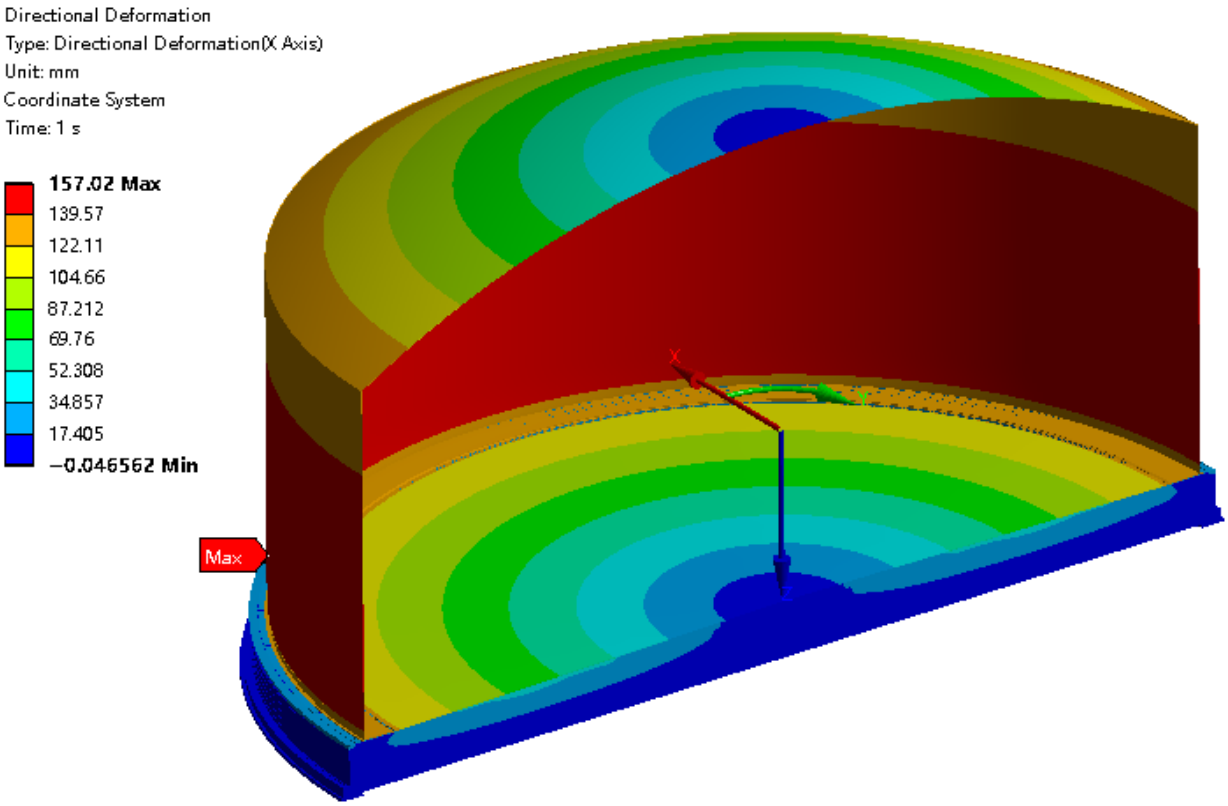


Figure 10. Radial deformation contour of the whole molten-salt tank.

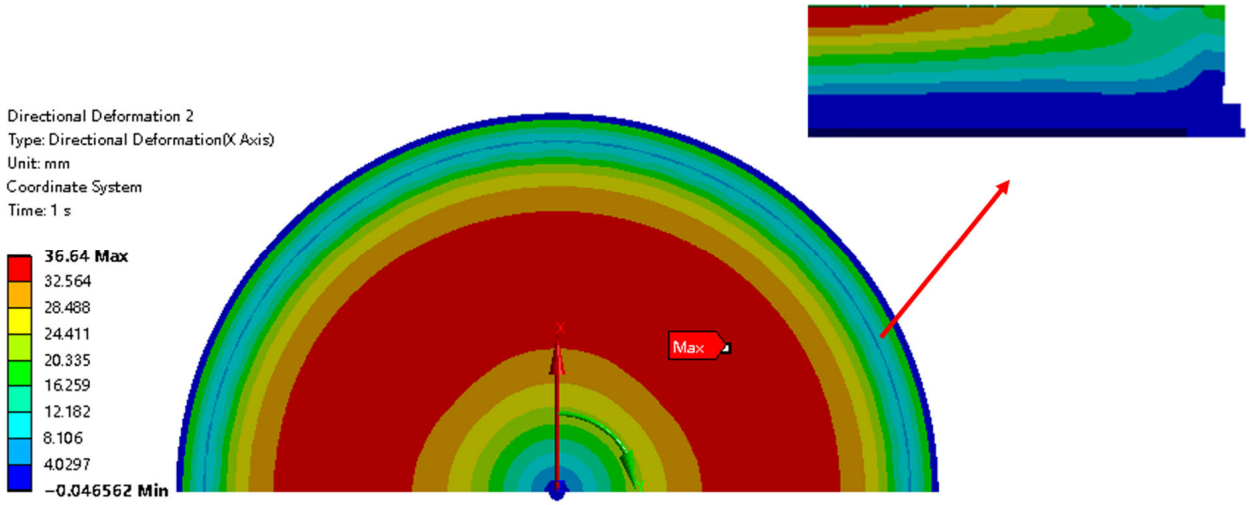


Figure 11. Dial deformation contour in the foundation of the molten-salt tank.

The height of the molten salt inside the tank may change during operation. To show the effect of molten-salt height variation, Table 5 lists the von Mises stress and radial deformation of the foundation at different molten-salt heights under constant internal pressure and operating temperature. Clearly, under the same internal pressure and operating temperature, the molten-salt height has no effect on the von Mises stress but significantly affects the radial deformation of the foundation.

Table 5. Von Mises stress and radial deformation of the foundation at different heights of molten salt.

Height of the Molten Salt (mm)	Maximum Von Mises Stress (MPa)	Maximum Radial Deformation (mm)
3000	229.1	12.72
6000	229.14	18.28
8000	229.17	24.13
12,000	229.26	36.64

4. Influence of the Ambient Temperature on the Temperature of the Foundation

During operation, the molten-salt tank may experience changes in ambient temperature. A good tank design should consider this situation and retain excellent insulation. Figure 12 shows the temperature distributions in the foundation at ambient temperatures of −28.7 °C, 0 °C and 20 °C, while the operating pressure is 0.002 MPa, the height of the molten salt is 12,000 mm and the operating temperature is 400 °C. It is seen that change in the ambient temperature from −28.7 °C to 20 °C has little effect on the temperature distribution in the foundation, meaning the tank insulation is very effective.

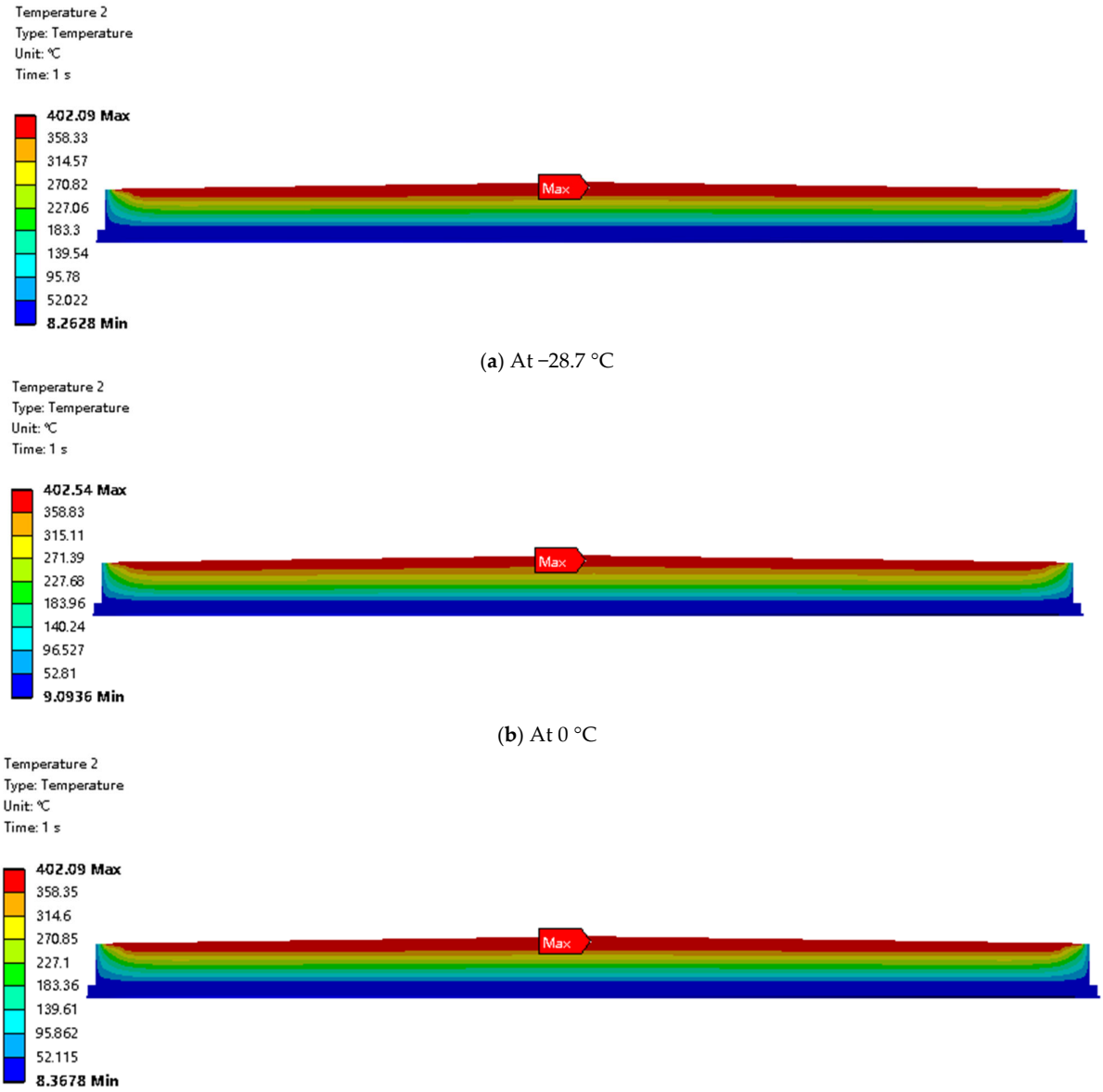


Figure 12. Temperature distribution in the foundation at different ambient temperatures.

5. Conclusions and Discussion

In this paper, a detailed numerical analysis of stress and deformation is conducted on the foundation of a large high-temperature molten-salt storage tank under realistic operating conditions, aiming to provide a relatively systematic and quantitative analysis of the thermo-mechanical coupling behavior of tank foundations with complex layered structures and material compositions, while also incorporating the impacts of actual service conditions. Based on the thermo-mechanical coupling analysis, the main conclusions are drawn as follows:

(1) The maximum von Mises stress occurring in the foundation is 229.26 MPa, which is located at the bottom steel plate of the tank. This result provides key quantitative data for the structural design and strength check of the tank foundation, making up for the deficiency of existing studies that mainly focus on the tank shell or overall structure rather than the foundation's stress characteristics.

(2) The radial deformation of the foundation was obtained, with the maximum value being 36.64 mm. This critical parameter is essential for the optimal design of the tank

foundation, as it directly reflects the foundation's bearing capacity and deformation resistance under actual service conditions (including the internal pressure, high-temperature molten salt, and ambient temperature variation), which were ignored in most previous investigations.

(3) Under the given internal pressure and operating temperature, the molten-salt height significantly affects the radial deformation of the foundation. This finding clarifies one of the key factors governing the performance of the tank foundation, providing targeted guidance for the safe operation and maintenance of large high-temperature molten-salt storage tanks.

(4) The change of the ambient temperature from −28.7 °C to 20 °C has little effect on the temperature distribution in the foundation, meaning that the tank insulation is very effective. This result verifies the rationality of the tank's insulation design and further supports the reliability of the proposed thermo-mechanical coupling analysis method under realistic operating conditions.

From this study, the following points can be generalized for engineering application:

(1) As the structure of the foundation of a high-temperature molten-salt storage tank is very complicated, numerical simulation for the design and safety assessment of the foundation is necessary and effective.

(2) To ensure the integrity of the molten-salt storage tank, the foundation should be constructed with multiple layers consisting of different materials, although the layer scheme may not be unique.

(3) For the numerical analysis of the foundation, the largest stress, largest deformation and temperature distributions are particularly important because these three indicators correspond to the strength, deformation and heat insulation of the foundation and are critical for the design and safety assessment of the tank.

Author Contributions: Conceptualization, J.Q., C.Q. and Z.W.; methodology, J.Q., C.Q. and Z.W.; software, J.Q. and Z.W.; validation, J.Q.; formal analysis, C.Q. and Z.W.; investigation, J.Q., C.Q. and Z.W.; resources, C.Q. and Z.W.; data curation, J.Q.; writing—original draft preparation, J.Q.; writing—review and editing, C.Q. and Z.W.; visualization, J.Q.; supervision, C.Q. and Z.W.; project administration, C.Q. and Z.W.; funding acquisition, C.Q. and Z.W. All authors have read and agreed to the published version of the manuscript.

Funding: This research received no external funding.

Data Availability Statement: The data presented in this study are available in article.

Conflicts of Interest: The authors declare no conflict of interest.

References

1. Islam, M.T.; Huda, N.; Abdullah, A.B.; Saidur, R. A comprehensive review of state-of-the-art concentrating solar power (CSP) technologies: Current status and research trends. *Renew. Sustain. Energy Rev.* **2018**, *91*, 987–1018. [CrossRef]
2. Saleh, M.; Jahromi, B.; Kalantar, V.; Samimi, H. Recent progress on solar cabinet dryers for agricultural products equipped with energy storage using phase change materials. *J. Energy Storage* **2022**, *51*, 104434. [CrossRef]
3. Starke, A.R.; Cardemil, J.M.; Bonini, V.R.; Escobar, R.; Castro-Quijada, M.; Videla, Á. Assessing the performance of novel molten salt mixtures on CSP applications. *Appl. Energy* **2024**, *359*, 122689. [CrossRef]
4. Wan, Z.; Wei, J.; Qaisrani, M.A.; Fang, J.; Tu, N. Evaluation on thermal and mechanical performance of the hot tank in the two-tank molten salt heat storage system. *Appl. Therm. Eng.* **2020**, *167*, 114775. [CrossRef]
5. Guo, H.; Zang, C.; Wang, Z.; Zhao, X.; Meng, Y.; Osorio, J.D.; Mehos, M. Analysis of thermal and mechanical properties with inventory level of the molten salt storage tank in central receiver concentrating solar power plants. *Appl. Therm. Eng.* **2025**, *260*, 124984. [CrossRef]
6. Zhang, X.; Wu, Y.; Ma, C.; Meng, Q.; Hu, X.; Yang, C. Experimental Study on Temperature Distribution and Heat Losses of a Molten Salt Heat Storage Tank. *Energies* **2019**, *12*, 1943. [CrossRef]

7. Klasing, F.; Schmitz, M.; Gerdes, C.; Odenthal, C.; Bauer, T. Critical diameter for a single-tank molten salt storage—Parametric study on structural tank design Freerk Klasing. *J. Energy Storage* **2024**, *101*, 113870. [CrossRef]
8. Ouyang, Y.; Li, Y.; Zhang, Y. Numerical research on the thermal characteristics and mechanical properties of a molten-salt single tank storage system. *J. Energy Storage* **2024**, *80*, 110328. [CrossRef]
9. Wang, G.; Yu, S.; Niu, S.; Chen, Z.; Hu, P. A comprehensive parametric study on integrated thermal and mechanical performances of molten-salt-based thermocline tank. *Appl. Therm. Eng.* **2020**, *17*, 113183. [CrossRef]
10. Tang, Z.; Tao, W.-Q. Strength analysis of molten salt tanks for concentrating solar power plants. *Energy Storage Sav.* **2023**, *2*, 571–577. [CrossRef]
11. Ren, B.; Zhu, C.; Li, B.; Tian, J.; Lu, Y.; Wang, Y. Thermal-mechanical coupling characteristics of large-scale molten salt storage tanks under stable operating conditions with varying liquid levels. *J. Energy Storage* **2024**, *100*, 113697. [CrossRef]
12. Xue, X.; Li, H.; Chen, C.; Wu, F.; Jin, K.; Ji, M.; Zhou, H. Thermal performance assessment and optimization simulation of large-scale molten salt storage tanks and foundation. *J. Energy Storage* **2025**, *109*, 115127. [CrossRef]
13. Jia, J.; Ma, Y.; Lu, Y.; Lv, S.; Li, Y.; Wu, Y. Numerical Analysis on Temperature Distribution and Heat Loss in the Large-Scale Molten Salt Storage Tank of CSP Plant. *Energy* **2025**, *335*, 137873. [CrossRef]
14. Wang, Y.; Liu, J.; Ma, X.; Ouyang, Y.; Zhu, D.; Zhang, Y. Solar energy materials and solar cells numerical investigation on the thermal performance of a molten salt tank under different electric heating method. *Sol. Energy Mater. Sol. Cells* **2024**, *278*, 113183. [CrossRef]
15. Tagle-Salazar, P.D.; Cabeza, L.F.; Prieto, C. Transient performance modelling of solar tower power plants with molten salt thermal energy storage systems. *J. Energy Storage* **2024**, *97*, 112793. [CrossRef]
16. Chen, C.; Liu, X.; Zhao, J.; Lan, Z.; Lin, Q.; Zhou, H. Study on Thermal and Mechanical Performance of Storage Tanks under Variations in Key Parametric Variables American Society of Mechanical Engineers. *Sol. Energy* **2026**, *309*, 114440. [CrossRef]
17. Du, B.; Guo, Y.; Xu, C.; Huang, L.; Li, X.; Lei, Y. Dynamic Creep and Stress Performances of the Packed-Bed Thermal Energy Storage Tank with Molten Salt EPCM Particles. *Appl. Therm. Eng. J.* **2023**, *225*, 120247. [CrossRef]
18. Gage, S.H.; Kesseli, D.; Dupree, J.; Kimbal, C.; Rigby, J.; Yates, J.; Morrison, B.; Bigham, G.; Turchi, C.S. Technical and economic feasibility of molten chloride salt thermal energy storage systems. *Sol. Energy Mater. Sol. Cells* **2021**, *226*, 111099. [CrossRef]

Disclaimer/Publisher's Note: The statements, opinions and data contained in all publications are solely those of the individual author(s) and contributor(s) and not of MDPI and/or the editor(s). MDPI and/or the editor(s) disclaim responsibility for any injury to people or property resulting from any ideas, methods, instructions or products referred to in the content.